ARTICLES

Structural Investigation of the Confinement of Finite Amounts of Trehalose in Water-Containing Sodium Bis(2-ethylhexyl)sulfosuccinate Reversed Micelles

C. Branca,*,† S. Magazù,† A. Ruggirello,‡ and V. Turco Liveri‡

Dipartimento di Fisica and INFM, Universita' di Messina, Post Office Box 55, Papardo, 98166 Messina, Italy, and Dipartimento di Chimica Fisica "F Accascina", Università di Palermo, Viale delle Scienze Parco D'Orleans II, 90128 Palermo, Italy

Received: July 17, 2006; In Final Form: October 4, 2006

The structural effect of trehalose confined in water-containing sodium bis(2-ethylhexyl)sulfosuccinate (AOT) reversed micelles at water to AOT molar ratio $W = 5$ and 10 as a function of the trehalose to AOT molar ratio T ($0 < T < 0.1$) has been investigated by small-angle neutron scattering (SANS). SANS data analysis is consistent with the hypothesis that trehalose is encapsulated within the quite spherical hydrophilic micellar cores of water-containing reversed micelles, causing an increase of the aggregate size and a decrease of the polydispersion. Moreover, SANS results suggest that the trehalose confinement in water-containing reversed micelles involves marked changes on the molecular packing of the water-containing micellar cores. In particular, according to the obtained findings, we can hypothesize the intercalation of the trehalose molecules between the polar surfactant headgroups. The preferential solubilization in this specific nanodomain could explain the trehalose capability to prevent, upon dehydration, the transition to a gel phase, hindering serious damage to biostructures.

Introduction

A huge amount of data accompanied by a parallel development of theories has been produced with regard to the confinement of finite amounts of a wide class of ionic, polar, and amphiphilic solubilizates in reversed micellar systems. This is because new and sometimes unexpected properties can be conferred on the entrapped species, and significant structural and dynamic changes of the hosting aggregates and of the entire system can be induced.[1,2] It follows that the confinement of opportunely selected molecules in solutions of reversed micelles has the possibility to generate complex liquid phases for specialized biological and technological applications. In particular, in view of the increasing interest toward industrial exploitation of disaccharide-based bioprotectors and of the ability of reversed micelles to model and/or to mime some fundamental aspects of biomembranes, their solubilization in water-containing reversed micelles is to be considered of utmost and current importance.[3] However, the knowledge in this field is limited and specifically the physicochemical characterization of reversed micellar systems containing bioprotectors as confined solutes is far from being satisfactory. This is due to the fact that only recently has the necessary attention been paid to the problem of bioprotection of food or biological materials of high added value by means of natural bioprotectors such as disaccharides.

In order to shed some light in this intriguing field, we have undertaken a systematic physicochemical investigation on the confinement of disaccharides in reversed micellar systems. In particular, aiming to unveil the structural perturbations caused by finite amounts of a representative molecule (trehalose) confined in the core of water-containing reversed micelles, here we report a small-angle neutron scattering (SANS) investigation on trehalose, D_2O/sodium bis(2-ethylhexyl) sulfosuccinate (AOT)/*n*-heptane system, performed as a function of the trehalose to AOT molar ratio (T) at a fixed AOT concentration (0.068 M) and two D_2O to AOT molar ratio values, W ($W = 5$ and 10).

We have chosen trehalose (α-D-glucopyranosyl-α-D-glucopyranoside) as representative of disaccharides because of its extraordinary effectiveness as a bioprotector in dehydration and freezing processes.[4−6] Trehalose, a nonreducing disaccharide of glucose, is commonly found in yeasts, spores, mushrooms, desert plants, and drought-adapted organisms. Experiments have revealed that these organisms are able to induce the production of trehalose as they desiccate, to survive in a "suspended" state, and then to resuscitate when rehydrated.[4−6] Disaccharides are also found to be effective cryoprotectors as they are able to maintain intact membrane structure at both high and low temperatures.[7−11] Even though disaccharides are currently the subject of an intense research effort, the molecular mechanisms underlying the bioprotective effectiveness of trehalose, whose characterization is basic for the understanding and exploitation of the potentialities of this disaccharide, have not yet been entirely understood.

AOT has been selected since it is one of the few surfactants able to form in apolar solvents, without the need of cosurfactants and in a large composition range, well-defined and widely investigated reversed micelles where a great amount of water or aqueous solution can be encapsulated.[12,13]

† Universita' di Messina.
‡ Università di Palermo.

10.1021/jp064512x CCC: $33.50
Published on Web 12/07/2006

SANS data have been analyzed by use of a hard-sphere interaction model and a Schultz distribution to take into account the particle polydispersity. Guinier's and Porod's laws were also used to obtain quantitative information on aggregate size, shape, interparticle interactions and geometrical parameters such as the surface area of the surfactant polar headgroups at the interface.

Experimental Section

Materials. Sodium bis(2-ethylhexyl)sulfosuccinate (AOT, Sigma, 99%) was dried under vacuum for several days before use. D-(+)-Trehalose (α-D-glucopyranosyl-α-D-glucopyranoside) dihydrate (Sigma, >99%), *n*-heptane (Aldrich, 99% spectrophotometric grade), and D_2O (Sigma, >99.96 atom % D) were used as received.

D_2O-containing AOT/*n*-heptane systems at various trehalose to AOT molar ratios T (T = [trehalose]/[AOT]) were prepared by adding the appropriate amount of D_2O/AOT/*n*-heptane solution, at fixed surfactant concentration ([AOT] = 0.068 M) and at two D_2O to AOT molar ratios (W = 5 and 10), to weighed quantities of trehalose. In order to extend our investigation to saturated samples, the solubility of trehalose was determined by visual inspection of samples prepared at various T values at constant temperature (25 °C). The thermodynamic solubility (i.e., in the presence of threalose crystals) in 0.068 M AOT/*n*-heptane at W = 5 and W = 10, expressed as the maximum trehalose to AOT molar ratio, is 0.06 and 0.09, respectively. It is worth noting that the solubilization of trehalose in D_2O/AOT/*n*-heptane solutions is itself proof of its entrapment in the heavy water-containing reversed micelles because its solubility in *n*-heptane is practically zero.

SANS Measurements. SANS measurements have been performed on the PAXE spectrometer of the Laboratoire Leon Brillouin at Saclay (France).

The SANS intensity was recorded as a function of the magnitude of the scattering vector $q = [4\pi \sin(\theta/2)]/\lambda$, where θ is the scattering angle and λ is the neutron wavelength equal to 5 Å with a wavelength spread $\Delta\lambda/\lambda < 10\%$. By varying the sample−detector distance, the available q range was between 3.27×10^{-2} and 3.95×10^{-1} Å^{-1}. The samples were contained in quartz cells and studied at a constant temperature of 25 ± 0.1 °C. Scattered neutrons were detected by a two-dimensional *XY* position detector with 64 × 64 active elements (BF_3) covering a total area of 4096 cm^2.

The collected spectra were normalized to transmission and sample path length. The intensity, corrected for the empty cell contribution, was normalized to absolute scale by a known cross-section standard. Data reduction was performed by using standard routines available at LLB.

Results and Discussion

In a SANS experiment, the normalized intensity of the radiation scattered by a collection of uniform monodispersed particles is given by

$$I(Q) = N_p P(Q) S(Q) \tag{1}$$

where N_p is the number density of scattering objects, $P(Q)$ is the intraparticle structure factor describing the normalized angular distribution of the scattering owing to the size and shape of the particle, $S(Q)$ is the structure factor that arises from interference effects due to spatial correlations between particles, and Q is the scattering vector. Assuming that aggregates interact through a hard-sphere potential, $S(Q)$ can be calculated by the Percus−Yevick approximation.

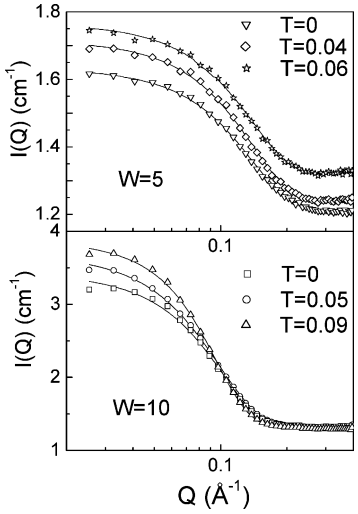

Figure 1. Scattering profiles and fitting curves of trehalose,D_2O/AOT/*n*-heptane microemulsions at the W and T values shown.

For homogeneous polydisperse spherical particles, the form factor $P(Q)$ is[14]

$$P(Q) = \int_0^1 f(R)|F(Q,R)|^2 \, dR \tag{2}$$

where $F(Q,R)$ is the particle form factor for a sphere of radius R that depends on the first-order spherical Bessel function $j_1(QR)$:

$$F(Q,R) = [3j_1(QR)/(QR)] \tag{3}$$

$f(R)$ is the normalized probability of a sphere having a total radius between R and $R + dR$.[14] The distribution that better describes the polydispersity in the micellar solutions is the Schultz distribution:[14]

$$f(R) = \left(\frac{z+1}{\bar{R}}\right)^{z+1} \frac{R^z}{\Gamma(z+1)} \exp\left(-\frac{z+1}{\bar{R}}R\right) \tag{4}$$

where $\bar{R}$ is the average radius of the particle, $\Gamma(z+1)$ is the gamma function, and z is the width parameter of the Schulz distribution ($z > 0$). z is related to the value of polydispersity, ξ, of the system as follows:

$$\xi = \frac{1}{\sqrt{z+1}} \tag{5}$$

Therefore, in considering a polydisperse particles system, the form factor $P(Q)$ spherically averaged can be developed in the Taylor series:

$$P(Q) = 1 - (Q\bar{R})^2/5 + \ldots \cong \exp[-\epsilon(Q\bar{R})^2/5] \tag{6}$$

where the parameter $\epsilon = [(z+8)(z+7)](z+1)^2$ is introduced to take into account the polydispersity.[14,15]

The SANS intensities for the samples at a fixed AOT concentration ([AOT] = 0.068 M), at W = 5 and 10 and various T values, are reported in Figure 1. The intensity rise observed by increasing T indicates that upon increasing the trehalose concentration the aggregates become larger, consistent with the hypothesis that the disaccharide is localized in the micellar aggregates. Because small-angle neutron scattering arises from

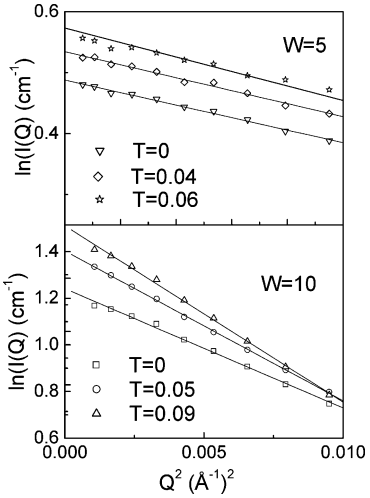

Figure 2. Plot of ln $I(Q)$ vs Q^2 of trehalose,D_2O/AOT/*n*-heptane microemulsions at the W and T values shown.

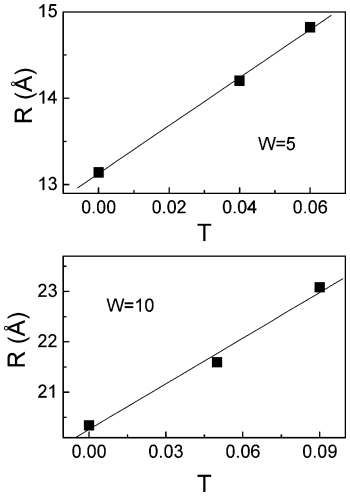

Figure 3. Linear plots of the micellar core radii as a function of T at $W = 5$ and 10.

the contrast between different adjacent domains, and when the peculiar structure and composition of D_2O-containing AOT reversed micelles are taken into account, the scattering centers are to be considered the hydrophilic micellar cores (water pools including trehalose plus the surfactant headgroup).[16]

A first evaluation of the micellar core dimensions has been performed through the Guinier plot of SANS data, that is, the natural logarithm of the scattered intensity plotted versus the square of the scattering vector, Q^2. In this representation the presence of a linear trend in the low Q region (see eq 6) can be used to obtain an estimate, neglecting polydispersity, of the radius of gyration, R_g:

$$R_g^2 = \frac{3\bar{R}^2}{5} \tag{7}$$

The results of the best fits to eq 6 are reported in Figure 2. For the samples at $W = 5$, the extracted radius of gyration varies from 5.3 ± 0.2 and 6.0 ± 0.2 Å by increasing T, whereas for the samples at $W = 10$ it increases from 12.3 ± 0.2 to 14.0 ± 0.2 Å. It is worthwhile to remember that the Guinier analysis by itself does not provide information on the shape of the scattering objects. However, from the trend of the radii of gyration, we can deduce that their size increases by increasing both the water content, as one can obviously expect, and the trehalose content.

To obtain more detailed information on the influence of trehalose on the structure and size of the micellar cores, we explored, as a first approach, the possibility to fit SANS data according to a model of monodisperse spheres or ellipsoids. However, these models were not able to reproduce our experimental SANS data. On the other hand, very nice fits were obtained by use of a model of interacting polydisperse hard spheres. The fits have been performed with the software IGOR PRO with radius $\bar{R}$, polydispersity, volume fraction, and background intensity as fitting parameters.

The fitting curves and fitting parameters obtained with this model are reported in Figure 1 and Table 1, respectively. It is worth noting that the mean radii of the AOT micellar cores at $W = 5$ and 10 and in absence of trehalose are in good agreement with those reported in the literature.[17]

Moreover, as one can see from an inspection of Table 1 and Figure 3, confirming previous conclusions obtained by the Guinier plot, by increasing the trehalose content the reversed micelles maintain a spherical shape; their size increases linearly

TABLE 1: Fitting Parameters Derived from Least-Squares Analysis of the SANS Data of the Trehalose,D_2O/AOT/*n*-Heptane Microemulsions

W	T	mean radius (Å)	polydispersity	vol fraction
5	0	13.1 ± 0.2	0.20	0.012
5	0.04	14.2 ± 0.2	0.15	0.012
5	0.06	14.8 ± 0.2	0.10	0.012
10	0	20.3 ± 0.2	0.17	0.02
10	0.05	21.5 ± 0.2	0.13	0.02
10	0.09	23.0 ± 0.2	0.11	0.02

whereas the polydispersity decreases. These findings are consistent with trehalose molecules being entirely confined in the micellar core, inducing swelling and stabilization of the reversed micelles.

In order to get more information from the T dependence of the mean micellar core radius, let us consider a simple geometric model based on the hypothesis, corroborated by the SANS data analysis, that water, trehalose, and surfactant headgroups form nanospheres whose surface is covered by a layer of about 8 Å constituted by the surfactant alkyl chains.[18]

Then, the volume V_{core} and the surface S_{core} of each nanosphere are given by

$$V_{core} = \frac{4\pi\bar{R}^3}{3} = n_{AOT}V_{AOT} + n_{D_2O}V_{D_2O} + n_{trehalose}V_{trehalose} \tag{8}$$

$$S_{core} = 4\pi\bar{R}^2 = n_{AOT}S_{AOT} \tag{9}$$

where n_{D_2O}, $n_{trehalose}$ and n_{AOT} are the number of molecules of D_2O, trehalose, and AOT in one micelle, V_{D_2O} and $V_{trehalose}$ are the molecular volumes of D_2O (32.7 Å^3) and trehalose, and S_{AOT} is the interfacial area of the AOT molecule at the core/alkyl chain interface. Combining eqs 8 and 9 and remembering that $W = n_{D_2O}/n_{AOT}$ and $T = n_{trehalose}/n_{AOT}$, one obtains

$$\bar{R} = \frac{3V_{AOT}}{S_{AOT}} + \frac{3V_{D_2O}W}{S_{AOT}} + \frac{3V_{trehalose}T}{S_{AOT}} \tag{10}$$

It follows that, in accord with our finding, the mean radius should linearly depend on the parameter T at constant W. Moreover, from the slopes of these trends and using eq 10 and $S_{AOT} = 52$ Å,[2,19] we obtained the following values of $V_{trehalose}$: 290 cm^3/mol at $W = 5$ and 311 cm^3/mol at $W = 10$. These

values are much greater than that of trehalose in water (210 cm^3/mol).[20,21]

When it is taken into account that the literature value includes the volume effects of trehalose on the water structure, the very high $V_{trehalose}$ values cannot be rationalized in terms of trehalose solubilization inside the water droplets. A more reasonable hypothesis is that the trehalose confinement in water-containing reversed micelles involves marked changes in the packing of the surfactant headgroups at the water/oil interface. In light of previous works,[22,23] these changes can be ascribed to the preferential intercalation of the trehalose molecules between the polar surfactant headgroups. From a biological point of view, in agreement with previous findings reported in literature,[24,25] this could explain why trehalose is able to prevent during drying the transition to a gel phase favoring a liquid crystalline one, preserving in such a way the integrity of biological structures.

Conclusions

From a SANS investigation of trehalose,D_2O/AOT/*n*-heptane microemulsions at two water to AOT molar ratios (*W*) and as a function of the trehalose to AOT molar ratio (*T*), it has been ascertained that the trehalose insertion within the aqueous core of AOT reversed micelles does not involve shape changes, while the mean core size increases linearly with the trehalose to AOT molar ratio. An analysis of these trends in terms of a simple geometrical model emphasizes the marked volume changes induced by trehalose encapsulation in the micellar cores. This allowed us to speculate that trehalose is not solubilized inside the water droplets but, as a consequence of a delicate equilibrium of specific intermolecular interactions, preferentially intercalated between the surfactant headgroups at the water/oil interface. This is consistent with the well-known capability of trehalose to preserve upon drying the integrity of biological structures. Because of the biological and technological relevance of this behavior, further investigations are planned to gain information on the peculiar state of finite amounts of trehalose confined in reversed micelles.

References and Notes

(1) Luisi, P. L.; Magid, L. J. *CRC Crit. Rev. Biochem.* **1986**, *20*, 4091.
(2) Turco Liveri, V. *Nano-Surface Chemistry*; Rosoff, M., Ed.; Marcel Dekker: New York, 2002; Vol. 1, p 473.
(3) Bongiorno, D.; Ceraulo, L.; Ferrugia, M.; Filizzola, F.; Ruggirello, A.; Turco Liveri, V. *J. Pineal Res.* **2005**, *38*, 292.
(4) Crowe, J. H.; Crowe, L. M. *Biological Membranes*; Academic Press: New York, 1984; p 57.
(5) Clegg, J. S. *Comp. Biochem. Physiol.* **1967**, *20*, 8.
(6) Elbein, A. D. *Chem. Biochem.* **1974**, *30*, 227.
(7) Green, J. L.; Angell, C. A. *J. Phys. Chem.* **1989**, *93*, 2880.
(8) Angell, C. A. *Hydrogen-Bonded Liquids*; NATO ASI Series, Series B, Vol. 329; Plenum: New York, 1991; p 59.
(9) Donnamaria, M. C.; Howard, E. I.; Grigera, J. R. *J. Chem. Soc., Faraday Trans.* **1994**, *90*, 2731.
(10) Leslie, S. B.; Israeli, E.; Lighthart, B.; Crowe, J. H.; Crowe, L. M. *Appl. Environ. Microbiol.* **1995**, *61*, 3592.
(11) Fox, K. C. *Science* **1995**, *267*, 1922.
(12) Eicke, H. F. In *Topics in Current Chemistry*; Boschke, F. L., Ed.; Springer-Verlag: New York, 1980; Vol. 87, pp 85−145.
(13) Yano, J.; Furedi-Milhofer, H.; Wachtel, E.; Garti, N. *Langmuir* **2000,** *16*, 9996.
(14) Kotlarchyk, M.; Chen, S. H. *J. Chem. Phys.* **1983**, *79*, 2461.
(15) Capuzzi, G.; Pini, F.; Gambi, C. M. C.; Monduzzi, M.; Baglioni, P. *Langmuir* **1997**, *13*, 6927.
(16) North, A. N.; Dore, J. C.; McDonald, J. A.; Robinson, B. H.; Heenan, R. K.; Howe, A. M. *Colloids Surf.* **1986**, *19*, 21.
(17) Gochman-Hecht, H.; Bianco-Peled, H. *J. Colloid Interface Sci.* **2005**, *288*, 230.
(18) Kotlarchyk, M.; Huang, J. S.; Chen, S. H. *J. Phys. Chem.* **1985**, *89*, 4382.
(19) Simmons, B.; Agarwal, V.; McPherson, G.; John, V.; Bose, A. *Langmuir* **2002**, *18*, 8345.
(20) Branca, C.; Magazu', S.; Maisano, G.; Migliardo, P. *J. Biol. Phys.* **2000**, *26*, 295.
(21) Miller, D. P.; dePablo, J. J.; Corti, H. *Pharm. Res.* **1997**, *14*, 578.
(22) Del C. Luzardo, M.; Amalfa, F.; Nunez, A. M.; Diaz, S.; Biondi de Lopez, A. C.; Disalvo, E. A. *Biophys. J.* **2000**, *78*, 2452.
(23) Viera, L. I.; Alonso-Romanowski, S.; Borovyagin, V.; Feliz, M. R.; Di salvo, E. A. *Biochim. Biophys. Acta* **1992**, *1145*, 157.
(24) Crowe, J. H.; Carpenter, J. F.; Crowe, L. M. *Annu. Rev. Physiol.* **1998**, *60*, 73.
(25) Crowe, J. H.; Leslie, S. B.; Crowe, L. M. *Cryobiology* **1994**, *31*, 355.